

## Noise Performance of Orthogonal RF Beamforming for THz Radio Communications

Krishan K. Tiwari<sup>1</sup>, SMIEEE, Eckhard Grass<sup>1,2</sup>, and Rolf Kraemer<sup>1,3</sup>

<sup>1</sup>IHP – Leibniz-Institut für innovative Mikroelektronik, Im Technologiepark 25, Frankfurt (Oder), Germany

<sup>2</sup>Humboldt-Universität zu Berlin

<sup>3</sup>BTU-Cottbus, Germany

Email: Krishan.Tiwari@ieee.org

**Abstract**—Ultra wide-band terahertz (THz) radio links are envisaged for high-throughput and low-latency radio communication from server to virtual reality (VR) head-mounted display (HMD). Orthogonal radio frequency (RF) beamforming is suitable for such extremely high-frequency radio links owing to the propagation characteristics. For RF beam training, the transmit-receive (Tx-Rx) beam combination yielding maximum received signal strength indication (RSSI) is selected. For complex signals employed in typical I/Q architecture communication systems, especially for THz frequencies, RSSI is Rayleigh-distributed. Receiver noise can cause false beam selections manifesting in communication rate loss. In this paper, analytically derived closed-form expressions and lower array dimension Monte Carlo (MC) simulation results for such noise performance evaluation have been presented.

**Index Terms**—Terahertz (THz) communications, Rayleigh-distributed RSSI, Orthogonal RF beamforming, Noisy RF beam training, Communication rate loss, Sparse MIMO channels.

### I. Introduction

Terahertz frequencies (0.1 to 10 THz) are being researched upon to alleviate the spectrum crunch for broadband wireless communications [1], [2], [3], [4]. Applications such as virtual reality (VR)/augmented reality (AR) are driving the exponentially increasing demand for terabits-per-second (Tbps) wireless connectivity in indoor spaces. Currently, VR head-mounted displays (HMDs) come along with heavy backpacks to be carried by the user. THz spectrum has the potential to provide high-throughput and low-latency radio communication from the VR server to HMDs thereby enabling the mobile users to enjoy VR/AR experience without carrying the backpack. VR/AR latency requirements are very strict in order to prevent cybersickness [5], [6]. Such THz radio communications for VR/AR applications rely on compact transceivers with very small form factors towards the ultimate goal of system-on-chip (SoC) realisation.

Using IHP's 130 nm SiGe BiCMOS technology, half wavelength dipole array configuration is one of the options for on-chip antenna array design.

Owing to higher free-space path loss (FSPL), higher atmospheric absorption, narrow beams, and small angle-spread multiple input multiple output (MIMO) channels at such high frequencies typically have only a few multipath components for communication i.e. such MIMO channels are sparse in beamspace [7], [8], [9]. Orthogonal RF beamforming is relevant for such systems due to its low power consumption, low cost, and low training overheads. Low power consumption is an extremely important advantage of analog beamforming for sparse MIMO channels in view the fact that the carbon footprint of information and communication technology (ICT) systems was as large as that of global air travel in 2008 [10]. The deployment of ICT systems has been growing since then and is highly likely to grow further in coming years.

For an  $N$  element uniform linear array (ULA),  $N$  orthogonal beams can be formed [11]. The beams are said to be orthogonal to each other if at the peak of one beam all other beams have their nulls. This minimises the spatial correlation or the inter-beam leakage among different beams. It is easier and more efficient to learn sparse THz MIMO channels in beamspace rather than in the spatial signal space [12]. Typically, the line-of-sight (LoS) is the dominant path for communication. For indoor scenarios, the angle spread is typically likely to be less than  $40^\circ$  [3]. For such applications, RF beam training is instrumental not only for quick Tx-Rx beam alignment but also for beam-based localisation. The work reported in this letter is relevant for any sparse MIMO communication system.

Multi-level beam selection [13], [14] is the state-of-the-art algorithm for RF beam training as compared to an exhaustive beam search since it offers significant savings in training overheads. For exhaustive beam search, all possible Tx-Rx beams combinations are tested for the maximum RSSI as seen in Figure 1. Whereas for multi-level beam search progressively nar-

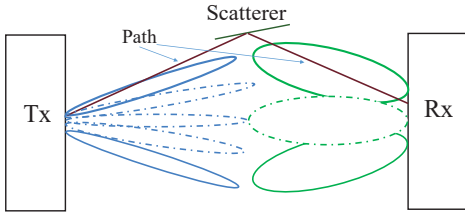


Figure 1. Illustration of Exhaustive RF beam search.

rower beams are used in multiple levels of beam training to search the best RSSI Tx-Rx beam combination only for the angular sector identified by the preceding level beam search as illustrated for only two levels at Tx in Figure 2 [13], [14]. Multi-level beam search is also known as hierarchical beam search or tree-based beam search.

The additive white Gaussian noise (AWGN) in the receiver can cause RSSI to be greater for a false beam combination as compared to the correct beam combination corresponding to actual multi-path component (MPC). Such false beam selections owing to receiver AWGN cause communication loss. Communication loss analysis in [12] assumed Gaussian distribution for RSSI. For complex Gaussian signals, as is commonly the case for I/Q i.e. quadrature receiver architecture, the beam selection is done on the basis of Rayleigh-distributed RSSI.

In context of such Rayleigh-distributed RSSI, this paper presents analytical derivations for the probability of correct beam training in presence of independent and identically distributed (i.i.d.) complex AWGN noise and mean communication rates on account of false beam selections for both exhaustive and multi-level RF beam-search techniques using orthogonal analog RF or intermediate frequency (IF) beamforming codebooks. The analog phase shifting can be implemented either at the final RF level or IF level or the local oscillator (LO) level. The presented results hold good for any of these implementations. Preliminary Monte Carlo (MC) simulation results validating the analytically derived closed-form expressions have also been presented.

The rest of the paper is organized as follows: Section II describes the system model, Section III specifies the problem statement, Section IV presents analytical derivations of closed-form expressions for the noise performances of the two RF beam-search algorithms, Section V presents Matlab simulation results, and Section VI summarises and concludes the paper.

The following notations have been used:  $\mathcal{X}$  is a matrix,  $\mathbf{x}$  is a vector,  $x$  is a scalar,  $\mathbf{C}^N$  is  $N$

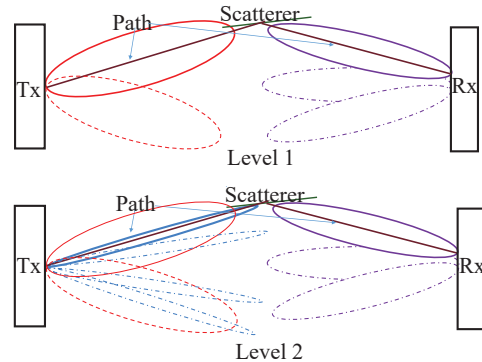


Figure 2. Illustration of Multi-level RF beam search [13], [14].

dimensional complex space,  $\sim$  denotes “distributed as”,  $x \sim \mathcal{N}(0, \sigma^2)$  is a complex Gaussian random variable with zero mean and  $\sigma^2$  as its variance,  $E[\cdot]$  is expectation operation,  $\|\mathbf{x}\|_2$  is 2-norm of vector  $\mathbf{x}$ ,  $|x|$  is magnitude of scalar  $x$ ,  $[\cdot]^*$  is conjugate transpose, and  $[\cdot]^T$  is transpose.

## II. System Model

We consider the scenario depicted in Figure 3. Let the transmitter and receiver have  $N_{TX}$  and  $N_{RX}$  antennas, respectively. We consider the beam training for one data-stream only and hence one RF chain each at the transmitter and the receiver. We assume narrowband block fading channel model. Orthogonal frequency division multiplexing (OFDM) can be used to convert broadband multi-tap channel to single-tap sub-channels. Let  $s \sim \mathcal{N}(0, \sigma_s^2)$  and  $n \sim \mathcal{N}(0, \sigma_n^2)$  be the transmitted signal for maximum mutual information and the receiver thermal AWGN noise, respectively. The  $N_{TX} \times 1$  radiated signal vector  $\mathbf{x}$  is given by equation (1),

$$\mathbf{x} = \mathbf{f}(\theta)s, \quad (1)$$

where  $\mathbf{f}(\theta)$  is the transmit analog RF beamforming vector for angle of departure (AoD)  $\theta$ . We consider orthogonal RF beamforming codebooks at transmitter as well as receiver. Orthogonal RF beamforming codebooks need only phase-shifts for beam steering and the aperture distribution is not changed [11]. This facilitates realisations using analog RF phase shifters with a constant modulus constraint as amplitude-control is not needed. Orthogonal beamforming codebooks have the advantage that they can be specified by a single parameter viz. the steering angle [11], [12]. For simplicity, the uniform linear array (ULA) has been considered at both transmitter and receiver. For steering the beam main response axis (MRA) to the direction  $\theta$ , the RF beamforming vector for an  $N$  element ULA is given by equation (2),

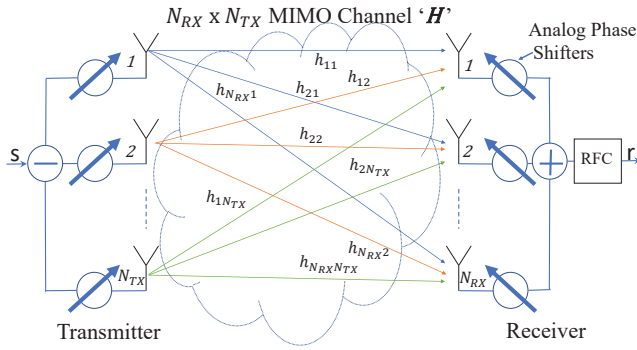


Figure 3. Tx-Rx System Model for Analog RF beamforming

$$\mathbf{f}(\theta) = [1; e^{-j\frac{2\pi}{\lambda} d \sin(\theta)}; \dots; e^{-j(N-1)\frac{2\pi}{\lambda} d \sin(\theta)}] / \sqrt{N}. \quad (2)$$

As seen in equation (2), entries of transmit beamforming codebook  $\mathcal{F}$  are normalised such that  $|\mathcal{F}_{m,n}|^2 = N_{TX}^{-1}$ , where  $\mathcal{F}_{m,n}$  indicates entry corresponding to the  $m^{th}$  row and  $n^{th}$  column of the RF precoder matrix  $\mathcal{F}$  having dimensions  $N_{TX} \times N_{TX}$  [12].  $N$  orthogonal beams can be formed with an  $N$ -element ULA. The MRAs in u-space corresponding to these  $N$  orthogonal beams are obtained by equations (3) and (4) for even and odd values of  $N$  respectively, where  $u_n = \sin(\theta_n)$  [11].

$$u_n = -1 + n \frac{2}{N}, \quad n = 0, 1, \dots, N-1 \quad (3)$$

$$u_n = -1 + \frac{1}{N} + n \frac{2}{N}, \quad n = 0, 1, \dots, N-1 \quad (4)$$

For orthogonal beamforming with ULAs, the transmit and receive RF beamforming codebooks  $\mathcal{F}$  and  $\mathcal{W}$  are unitary discrete Fourier transform (DFT) / Butler matrices as in equations (5) and (6), respectively.

$$\mathcal{F}\mathcal{F}^* = \mathcal{F}^*\mathcal{F} = \mathbf{I}_{N_{TX}} \quad (5)$$

$$\mathcal{W}\mathcal{W}^* = \mathcal{W}^*\mathcal{W} = \mathbf{I}_{N_{RX}} \quad (6)$$

Under ideal conditions i.e. in the absence of receiver AWGN noise, the received signal  $y$  at the output of the receiver RF chain is given by equation (7),

$$y = \mathbf{w}(\phi) \mathbf{H} \mathbf{f}(\theta) s, \quad (7)$$

where  $\mathbf{w}(\phi)$  is the receiver RF beamforming / combining vector of size  $N_{RX} \times 1$  for angle of arrival (AoA)  $\phi$ . We assume channel matrix  $\mathbf{H}$  to be of rank one due to single MPC.

### III. Problem Statement

Due to the orthogonality of beams, ideally the receiver output should be zero for incorrect beam combinations. RSSI should be largest for the correct Tx-Rx beam combination corresponding to the available MPC in which case the desired signal power will be detected at the receiver output. Maximum RSSI occurs when  $\mathbf{w}(\phi)$  and  $\mathbf{f}(\theta)$  point along the available MPC angle of arrival (AoA)  $\phi_r$  and angle of departure (AoD)  $\theta_t$ , respectively. In such cases, maximum beamforming gain  $G = N_{TX} \times N_{RX}$  will be realised. If there are angular offsets, scalloping loss [15] will be observed. For analytical simplicity and without the loss of generality, we assume the former condition such that the combined beamforming gain ( $G$ ) is equal to  $N_{RX} \times N_{TX}$ .

In practical conditions, the thermal noise will be present in the receiver. Due to the receiver AWGN noise, the receiver output of equation (7) gets modified as in equation (8),

$$r = y + n = \mathbf{w}(\phi) \mathbf{H} \mathbf{f}(\theta) s + n. \quad (8)$$

The transmit and receive beams are selected for the largest RSSI  $q = |r|$  as in equations (9) and (10), respectively.

$$\theta_t = \operatorname{argmax}_{\theta} q \quad (9)$$

$$\phi_r = \operatorname{argmax}_{\phi} q \quad (10)$$

The signal-to-noise ratio ( $SNR$ ) at the receiver is given as  $SNR = \sigma_s^2 / \sigma_n^2$ . The noise may cause the RSSI to be larger for Tx-Rx beam combination not corresponding to the actual MPC. These events of false beam selections cause communication rate loss. It is of practical significance to quantify such communication rate loss for both exhaustive and multi-level beam search techniques.

### IV. Analytical Derivations

We derive closed-form expressions for the Exhaustive beam search first in subsection IV.I and then for the Hierarchical beam search in subsection IV.II.

#### IV.1. Exhaustive Beam Search

Since the noise is i.i.d., the probability of the correct beam training by selecting correct Tx-Rx beam combination, from  $N_{TX} \times N_{RX}$  possible beam combinations, corresponding to the MPC of the channel such that RSSI  $q$  is maximised can be given by the product of probabilities for  $(N_{TX} \times N_{RX}) - 1$  pairwise correct beam selections. The problem thus reduces to a two-dimensional scenario.

We ignore FSPL and other attenuations for the notational simplicity of this statistical analysis. Thus, for correct beam selection, receiver output signal  $r \sim \mathcal{N}(0, \sigma_r^2 = G \times \sigma_s^2 + \sigma_n^2)$  which contains both the desired signal and the noise,  $G = N_{RX} \times N_{TX}$  is the total beamforming gain. So, for the correct beam selection,  $C = |r|$  is Rayleigh-distributed with its probability density function (pdf) given by equation (11),

$$f_C(c) = \frac{c}{\sigma_r^2} e^{-c^2/2\sigma_r^2}. \quad (11)$$

For false beam selections, receiver output  $r_w \sim \mathcal{N}(0, \sigma_n^2)$  with unitary beamforming codebooks.  $W = |r_w|$  is Rayleigh-distributed with its pdf given by equation (12),

$$f_W(w) = \frac{w}{\sigma_n^2} e^{-w^2/2\sigma_n^2}. \quad (12)$$

The bivariate probability density function for the two independent random variables  $C$  and  $W$  is given by equation (13),

$$\begin{aligned} f_{C,W}(c, w) &= f_C(c) f_W(w) \\ &= \frac{cw}{\sigma_r^2 \sigma_n^2} e^{-c^2/2\sigma_r^2} e^{-w^2/2\sigma_n^2}. \end{aligned} \quad (13)$$

Going by the single-shot measurement principle due to rapidly changing channel, we take only one random sample  $c$  and  $w$  each from  $C$  and  $W$ , respectively. The probability of  $c > w$  is given by equation (14),

$$\begin{aligned} P(c > w) &= \int_0^\infty \int_0^c f_{C,W}(c, w) dw dc \\ &= \int_0^\infty \frac{c}{\sigma_r^2} e^{-c^2/2\sigma_r^2} \int_0^c \frac{w}{\sigma_n^2} e^{-w^2/2\sigma_n^2} dw dc \\ &= \int_0^\infty \frac{c}{\sigma_r^2} e^{-c^2/2\sigma_r^2} \mathcal{A} dc, \end{aligned} \quad (14)$$

where  $\mathcal{A}$  is given by equation (15),

$$\mathcal{A} = \int_0^c \frac{w}{\sigma_n^2} e^{-w^2/2\sigma_n^2} dw = 1 - e^{-c^2/2\sigma_n^2}. \quad (15)$$

Substituting equation (15) in equation (14) gives equation (16),

$$\begin{aligned} P(c > w) &= \int_0^\infty \frac{c}{\sigma_r^2} e^{-c^2/2\sigma_r^2} (1 - e^{-c^2/2\sigma_n^2}) dc \\ &= 1 - \frac{\sigma_n^2}{\sigma_r^2 + \sigma_n^2} = 1 - \frac{\sigma_n^2}{G \times \sigma_s^2 + 2\sigma_n^2} \\ &= 1 - \frac{1}{G \times \sigma_s^2 / \sigma_n^2 + 2} = 1 - \frac{1}{2 + G \times SNR}, \end{aligned} \quad (16)$$

where  $SNR = \sigma_s^2 / \sigma_n^2$ .

$P(c > w)$  of equation (16) gives the probability of correct beam training for only two beam combinations. We noted earlier that for  $N_{TX} \times N_{RX}$  beam combinations, the probability of overall correct beam training is given by the product of  $N_{TX} \times N_{RX} - 1$  pairwise correct beam selections due to their independence. So, the probability of overall correct beam training  $P_{cbt}$  is given by equation (17),

$$P_{cbt} = \left[ 1 - \frac{1}{2 + G \times SNR} \right]^N, \quad (17)$$

where  $N = G - 1$ .

The mean communication rate  $\bar{R}$  (bps/Hz) for noisy beam training is given by equation (18),

$$\bar{R} = P_{cbt} R, \quad (18)$$

where  $R = \log_2(1 + G \times SNR)$  is the communication rate with ideal beam training i.e. without any false beam selections due to receiver noise.

The above derivation assumed that there is only one MPC which corresponds to a correct pair of Tx-Rx beams. For more than one MPC, the beam combination yielding maximum RSSI will be given to the first stream/MPC. While doing the beam training for the first MPC/data-stream, remaining MPCs' RSSIs will also be Rayleigh-distributed but with higher power as compared to the beam combinations which have no MPC and give only the receiver noise at the output. Thus, the analysis holds good for multi-MPC scenarios as well with only trivial difference that due to higher variance for a few other beam combinations, the probability of correct beam training will be lower for the initial MPC as compared to the single MPC scenario. For THz communications, the first-order and second-order reflected MPCs are typically 5-10 dB and more than 15 dB weaker than the LoS MPC, respectively [3], [4]. Since less number of beam combinations will be tested for subsequently trained MPCs/data-streams, chances of false beam selections will be lower for subsequent beam selections due to reduced exponent in equation (17).

## IV.2. Multi-level Beam Search

For multi-level beam search, let  $k$  be the number of beam-search levels both at the transmitter and the receiver for simplicity. For given  $N_{TX}$  and  $N_{RX}$ ,  $k$  should be chosen such that it is an integer as it is the number of levels for the hierarchical beam search. For the first level, all possible combinations of  $b_t$  transmit beams and  $b_r$  receive beams will be tested for maximum RSSI i.e.  $k_1 = b_t \times b_r - 1$  beam-combination pairs will be tested where  $b_t$  and  $b_r$  are  $k^{th}$  roots of  $N_{TX}$  and  $N_{RX}$ , respectively. If transmitter and receiver employ different numbers of beam-search levels, say  $k_t$  and  $k_r$ , respectively, then  $b_t$  and  $b_r$  will be  $k_t^{th}$  and

$k_r^{th}$  roots of  $N_{TX}$  and  $N_{RX}$ , respectively. Since the access node typically can have much larger number of antenna elements as compared to HMD,  $k_t > k_r$ . In those cases, the receive beam selected for  $k_r^{th}$  level will be used for higher levels of transmit beam search. For notational simplicity and with only trivial changes otherwise, we go ahead with  $k_t = k_r = k$ .

Since unitary beamforming codebooks are used,  $k_2 = (b_t + 1) \times (b_r + 1) - 1 = k_1 + b_t + b_r + 1$  beam combinations will be tested for second and further levels to include beams at both edges of the respective sector. The receiver noise power remains the same for all the levels. The signal and noise statistics are the same as for the exhaustive beam search. The beamforming gain will be smallest for the first level and progressively increase for subsequent levels due to increasing number of switched-on antenna array elements. The combined BFG for different levels will be  $G/(b_t b_r)^{k-j}$  where  $j$  is the beam search level number. Thus, the probability for overall correct beam training for tree-based beam search is given by equation (19),

$$P_h = \left[ 1 - \frac{1}{2 + SNR \times G / (b_t b_r)^{k-1}} \right]^{k_1} \times \prod_{j=2}^{j=k} \left[ 1 - \frac{1}{2 + SNR \times G / (b_t b_r)^{k-j}} \right]^{k_2}. \quad (19)$$

Equation (18) remains valid with  $P_{cbt}$  replaced by  $P_h$ .

For  $N_{TX} = 64$ ,  $N_{RX} = 8$  and  $k = 3$ , we get  $N = 511$  and  $K = k_1 + k_2 \times (k - 1) = 35$  for exhaustive and multi-level beam searches for the first stream, respectively.  $N$  and  $k_1, k_2$  are the exponents in equations (17) and (19), respectively. Since  $N \gg K$ , we see that noise gets much less chances of causing false beam selections for multi-level beam search as compared to exhaustive beam search. Hence, much higher mean communication rates are achievable with the hierarchical RF beam training than with exhaustive beam search. We see that in addition to savings in training overheads as reported prior to this paper, tree-based beam search also offers huge savings in communication loss due to false beam training owing to receiver AWGN noise.

## V. Simulation results

The graphical visualisation of receiver thermal noise causing false beam selections is evident from Figure 2 of [12], reproduced here as Figure 4 for convenience. In absence of noise i.e. with ideal beam training all beam combinations, except  $9^{th}$  Tx beam and  $3^{rd}$  Rx beam highlighted by a marker in the figure, should have produced zero output at the receiver due to orthogonality of the beams. However, random

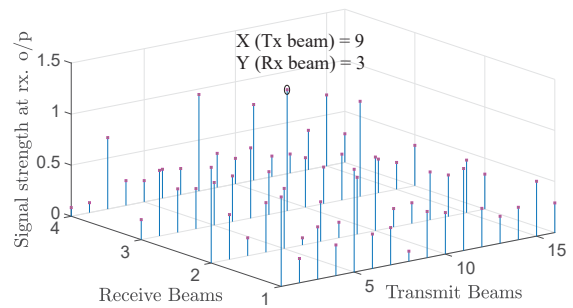


Figure 4. Noisy exhaustive beam search;  $N_{RX} = 4$   $N_{TX} = 16$  [12].

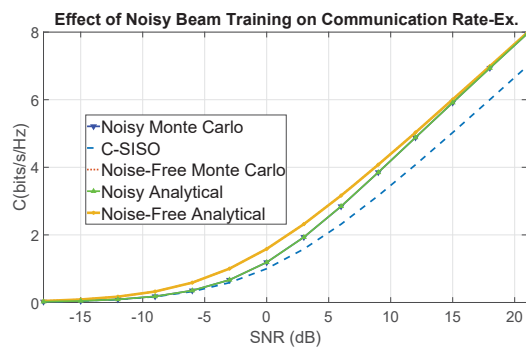


Figure 5. Performance comparisons;  $N_{RX} = 1$   $N_{TX} = 2$ .

and finite receiver output power levels or RSSIs are sensed for all non-MPC beam-combinations due to noise as seen in the figure. Such noisy false RSSIs can get higher than the desired/true signal-plus-noise RSSI for correct beam-combination leading to false beam selection which doesn't correspond to an actual MPC manifesting as communication loss during the data communication phase.

Reference [12] brought out that, with increasing MIMO dimensions, noise performance of tree-based beam search approaches exponentially and asymptotically that of ideal beam training by virtue of cutting down the number of beam-combinations to be tested for maximum RSSI as compared to exhaustive beam search. The result holds good even for RF beam training based on Rayleigh-distributed RSSI as only the expression for probability of pairwise correct beam training changes in our analysis in section IV.

MC simulations have been completed for lower array dimensions. As seen in Figure 5, noisy MC simulation results match very closely with analytical results for noisy exhaustive beam search for low dimension multiple input single output (MISO) cases. Similar, results are obtained for low dimension single input multiple output (SIMO) cases as well. The difference curve between analytical rates and MC simulation rates for noisy RF beam training has been explicitly plotted

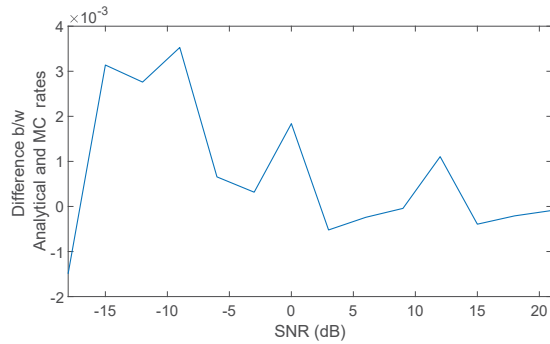


Figure 6. Difference b/w Analytical and MC simulation results.

in Figure 6. As seen in Figure 6, a negligibly small difference is observed due to the statistical noise of MC simulations. The rate difference is negative at some points due to rounding/truncation errors as well.

## VI. Conclusions

For commonly used I/Q i.e. quadrature receiver architectures which use Rayleigh-distributed RSSI, closed-form expressions have been derived for mean communication rates for noisy exhaustive and hierarchical beam searches employing orthogonal RF beamforming codebooks. The analytical results have been validated by MC simulations for low dimensional MISO/SIMO cases. MC simulations need to be further performed to validate the analytical results for general high-dimensional MIMO cases. It is also planned to practically validate the results using 240 GHz beamforming chips of IHP.

## Acknowledgment

This work has received funding from the European Union's Horizon 2020 research and innovation programme under grant agreement No 761329.

## References

- [1] R. Piesiewicz et al., "Short-Range Ultra-Broadband Terahertz Communications: Concepts and Perspectives," *IEEE Antennas and Propagation Magazine*, vol. 49, no. 6, pp. 24-39, Dec. 2007.
- [2] K. Huang and Z. Wang, "Terahertz Terabit Wireless Communication," *IEEE Microwave Magazine*, vol. 12, no. 4, pp. 108-116, June 2011.
- [3] S. Priebe and T. Kürner, "Stochastic Modeling of THz Indoor Radio Channels," *IEEE Transactions on Wireless Communications*, vol. 12, no. 9, pp. 4445-55, Sept. 2013.
- [4] I. F. Akyildiz, J. M. Jornet, and C. Han, "Terahertz Band: Next Frontier for Wireless Communications," *Phys. Commun.*, vol. 12, no. 2, pp. 16-32, Sept. 2014.

- [5] EU WORTECS Consortium, "European Union's Horizon 2020 research and innovation programme under grant agreement No 761329 WORTECS project website," [Online]. Available: <https://worteecs.cms.orange-labs.fr/node/18> [Accessed: 10-Nov-2018].
- [6] M. Badawi et. al, "EU H2020 WORTECS Deliverable D2.3: Focus on Virtual Reality," [Online]. Available: <https://worteecs.cms.orange-labs.fr/node/18/deliverables-dissemination> [Accessed: 10-Nov-2018].
- [7] A. M. Sayeed, "Deconstructing multiantenna fading channels," *IEEE Transactions on Signal Processing*, vol. 50, no. 10, pp. 2563-2579, Oct. 2002.
- [8] A. Sayeed and J. Brady, "Beamspace MIMO for high-dimensional multiuser communication at millimeter-wave frequencies," *IEEE Global Communications Conference (GLOBECOM)*, Atlanta, GA, pages 3679-3684, Dec. 2013.
- [9] G. H. Song, J. Brady, and A. Sayeed, "Beamspace MIMO transceivers for low-complexity and near-optimal communication at mm-wave frequencies," *IEEE International Conference on Acoustics, Speech and Signal Processing (ICASSP)*, Vancouver, BC, pages 4394-4398, May 2013.
- [10] G. P. Fettweis and E. Zimmermann, "ICT Energy Consumption-Trends and Challenges," *The 11th International Symposium on Wireless Personal Multimedia Communications (WPMC 2008)*, Lapland, Finland, pages 1-4, Sept. 2008.
- [11] H. L. V. Trees, *Optimum Array Processing: Part IV of Detection, Estimation, and Modulation Theory*, New York: Wiley-Interscience, 2002.
- [12] K. K. Tiwari, J. S. Thompson, and E. Grass, "Noise performance of Orthogonal RF beamforming for millimetre wave massive MIMO communication systems," *The Tenth International Conference of Wireless Communications and Signal Processing (WCSP)*, Hangzhou, China, Oct. 2018.
- [13] S. Hur, T. Kim, D. J. Love, J. V. Krogmeier, T. A. Thomas, and A. Ghosh, "Multilevel millimeter wave beamforming for wireless backhaul," *IEEE GLOBECOM Workshops (GC Wkshps)*, Houston, TX, pages 253-257, Dec. 2011.
- [14] S. Hur, T. Kim, D. J. Love, J. V. Krogmeier, T. A. Thomas, and A. Ghosh, "Millimeter Wave Beamforming for Wireless Backhaul and Access in Small Cell Networks," in *IEEE Transactions on Communications*, vol. 61, no. 10, pp. 4391-4403, Oct. 2013.
- [15] K. K. Tiwari, "Beamforming Techniques for Millimetre Wave Communications," section 3.9, *M. Sc. thesis, matriculation number s1113092*, The University of Edinburgh, Edinburgh, U.K., Aug. 2017.